

1                   **Tradeoff-mediated Drought Legacy in Soil Microbiome**

2

3   **Abstract**

4         The irreplaceable, profound role of soil microbiome in completing biogeochemical cycling  
5         in the Earth System makes fully understanding its response to drought of increasing frequency and  
6         severity pivotal toward evaluating drought-mediated biosphere-atmosphere interactions. Though  
7         with over a-half century of extensive research on drought impacts on soil microbiomes, drought  
8         legacy, a phenomenon of persistence of past effects that has been widely discussed in soil  
9         microbiome (and broadly across natural systems) and may largely influence microbiome and  
10        ecosystem functioning, is still with a yet unresolved mechanism. Here, using a trait-based  
11        microbial systems modelling framework with an explicit intra-cellular metabolic allocation of  
12        enzyme (A), osmolyte (S), and yield (Y), we revealed a range of drought legacy scenarios from  
13        persistent through transient to no legacy depending on drought intensity and microbial dispersal.  
14        These trait-based findings point to a more fundamental physiological tradeoff-based and  
15        community position-determined mechanism. This mechanism indicates that any factor that can  
16        influence the physiological tradeoff between resource acquisition (i.e., enzymes) and stress  
17        tolerance (e.g., osmolytes) and change the trajectory of a community on the enzyme investment-  
18        drought tolerance-yield constrained space would alter the property of drought legacy. These  
19        mechanistic insights into historical contingency of soil microbiome functioning hold tremendous  
20        promise to quantifying and predicting soil microbiome functioning more accurately. This study  
21        inspires us to couple microbiome with vegetation with a holistic ecosystem view by capturing  
22        major tradeoff dimensions to evaluate and predict drought-biosphere interactions.

23

24      **1 Introduction**

25      Drought of increasing severity and frequency both regionally and worldwide (**Borsa et al.**  
26      **2014; Park Williams et al. 2020**) is one of the most pressing problems to the biosphere in general  
27      and to, specifically, microbiome in terrestrial ecosystems (**Berdugo et al. 2020**). The unparalleled  
28      role of soil microbiome in driving materials' cycling in the Earth system (**Falkowski et al. 2018**)  
29      makes understanding its response to drought integral for systematically evaluating drought impacts  
30      on the biosphere, which, however, is still largely missing or implicitly treated in global assessments  
31      of drought-biosphere interactions (e.g., **Green et al. 2019**). Over a-half century of research has  
32      uncovered physio-chemical, physiological, and ecological mechanisms explaining immediate  
33      impacts of drought on microbial systems functioning in soil environment (e.g., **Birch 1958,**  
34      **Schimel 2007; Manzoni et al. 2012**). However, persistence of drought effects in soil microbiome  
35      (e.g., **Evans and Wallenstein 2012; Meisner et al. 2015; Hawkes et al. 2017; Hinojosa et al.**  
36      **2019; Glassman et al. 2019**), a phenomenon termed drought legacy that has also been widely  
37      observed across the forest biome (e.g., **Anderegg et al. 2015; Johnstone et al. 2016; Conradi et**  
38      **al. 2020**), still intrigues researchers for mechanistic explorations. Elucidating the processes leading  
39      to drought legacy in organic matter decomposition is undoubtedly not only essential for  
40      understanding microbial systems resilience but also for completely quantifying responses and  
41      feedbacks of whole ecosystems to drought in the Earth System.

42      Past lab- and field-based efforts on soil microbiome drought legacy, though having made  
43      huge, inspiring progress, are still far from being conclusive both mechanistically and conceptually.  
44      Those studies remained at the stage of loosely depicting compositional differences in terms of a  
45      few functional types. Notably, **Hawkes and Keitt (2015)** proposed a mechanism of community-  
46      level shift in relative abundance of moisture generalist vs. specialist, of which generalist is

**Commented [SDAI]:** I think there is too much covered in this paragraph. I suggest one paragraph on the importance/prevalence of drought, another on the impacts on microbiomes and C cycling, and then a third that introduces the legacy definition and concept.

**Commented [BW2R1]:** This structure totally makes sense to me.

But I'm also thinking it might not be worth using too much ink on drought and carbon cycling, especially in separate paragraphs. Instead, do you think it would be better to directly introduce to the reader the research topic, legacy, and point out the problem, mechanism, in the very 1st paragraph?

If you do not agree with this arrangement, then I'm happy to revise it as you suggested.

47 functionally more stable than specialists with moisture. This idea was argued to explain the  
48 observation of a lack of change in moisture response across sites in Texas, USA because of  
49 observed dominance by generalist taxa resulting from high variation in historical rainfall (**Hawkes**  
50 **et al. 2017; Waring and Hawkes 2018**). Similarly, **Evans and Wallenstein (2014)** argued from  
51 the point of view of discrete life strategy to explain soils with relatively stable moisture history  
52 had more moisture-sensitive taxa and hence larger changes in biomass and composition (**Evans**  
53 **and Wallenstein 2012**). These proposed explanations at the community level in terms of coarse,  
54 discrete functional groups, though intuitively appealing, cannot really tell how a community can  
55 be really shaped by past drought disturbance and how its functional change can persist to enable  
56 drought legacy. This deficiency becomes especially apparent when having many studies reporting  
57 legacies of varying magnitudes with differing time frames, especially those that even did not  
58 observe a drought legacy at all (e.g., **Rousk et al. 2013; Fuchslueger et al. 2016**). In fact, such a  
59 missing of mechanistic details also applies to warming-based historical contingency of microbial  
60 systems functioning (e.g., **Karhu et al. 2014**). We need a more fundamental mechanistic  
61 explanation that can link individual-level mechanistic details to community-level interactions to  
62 explain persistence of microbial systems functioning. Moreover, in a field manipulative  
63 experiment of rainfall and nitrogen conducted at Loma Ridge, Southern California, **Martiny et al.**  
64 (**2017**) measured drought legacy attributed to bacterial composition change with an alteration of  
65 carbohydrate degradation traits but not for nitrogen addition that instead did not present a change  
66 in carbohydrate degradation traits. This clear contrast further motivates us to find a trait-based  
67 linkage between organismal physiology and community shift underlying legacy.

68 Trait-based insights can bridge the gap between individual physiology and community-  
69 level dynamics, which are expected to explain the drought legacy phenomenon. Physiologically,

it is well established that a microbial cell can direct available resources from producing exoenzymes to acquire resources to produce, e.g., osmolytes, to combat desiccation (e.g., **Schimel 2007**), an intra-cellular metabolic plasticity responding to fluctuating environment that displays large inter-cellular variability (e.g., **Manzoni et al. 2012**). Quantifying the individual-level metabolic variation in these processes using physiological traits that reflect and determine demographic variation among individuals, a trait-based mechanistic framework, Y-A-S (Yield-Acquisition-Stress), has been proposed (**Malik et al. 2019**). Therefore, in response to drought pressure physiological adaptation and turnover of individuals comprising a microbial community would drive community-level changes against the need to increase its community-level drought tolerance. Unambiguously, a drought legacy of changing organic matter decomposition can be induced only by persistence of the functional change of a microbial community; a legacy may occur if an emergent community trade off its increased drought tolerance with decreased enzyme investment. With this reasoning any factor that can eventually modify such a tradeoff from the bottom up may alter the property, magnitude, and duration of drought legacies. For instance, the intensity of drought, which directly modulates intracellular metabolic allocation (**Csonka 1989**; **Schimel 2007**), may shape the tradeoff. In addition, dispersal of microbes, a pivotal process in microbial community assembly by introducing taxa with different trait values (e.g., **Fukami 2015**; **Vila et al. 2019**), is another factor that may alter drought legacy (**Hawkes et al. 2017**). To uncover this trait-based mechanism underpinning and factors influencing drought legacy in microbiome, it is methodologically intrinsic to employ a bottom-up approach that can integrate trait-based individual-level mechanistic details and community-level interactions into microbial systems functioning, which hinders lab- and field-based studies.

92 Instead, theory-driven trait-based modelling is well positioned to transcend limitations  
93 embedded in the current generation of lab- and field-based investigations. Individual-based  
94 microbial system modelling applying a trait-based approach is able to bridge across scales from  
95 individual cell through community to the system level to explicitly simulate ecological dynamics  
96 of microbial communities and emergent functioning. Such a modelling approach is superior to the  
97 prevailing aggregated modelling approach of treating microbes as a single biomass pool or a few  
98 discrete functional groups [a review by **Wieder et al. (2015); Hawkes and Keitt (2015)**]. It offers  
99 a flexible modelling framework allowing building trait-based intra-cellular metabolic processes  
100 into it and incorporating the tremendous taxonomic diversity, as well as examining microbial  
101 dispersal (**Allison 2012**). Moreover, conducting modelling of legacy can directly test the claim  
102 that including legacy would be trivial in biogeochemical modelling (**Rousk et al. 2013**).

103 Is the trait-based, tradeoff-mediated mechanism underpinning soil microbiome drought  
104 legacy? This study addressed this overarching question using a mechanistically and spatially  
105 explicit trait- and individual-based soil microbial systems modelling framework—DEMENTpy.  
106 Specifically, these following questions were answered: how does the magnitude of drought legacy  
107 effects on decomposition vary with drought intensity? How does dispersal of microbes affect the  
108 formation of drought legacy? And what are the underlying changes in traits of enzyme investment  
109 and drought tolerance? We tackled these questions by applying the DEMENTpy to a grassland  
110 ecosystem in Southern California. This study would open up rich possibilities for more quantitative  
111 investigations into trait-based rules of soil microbial community assembly and into implications  
112 of legacies in microbial systems interacting with vegetation activities for the biosphere-atmosphere  
113 interactions.

114

115    **2 Methods**

116    **2.1 Model description**

117        DEMENTpy (DEcomposition Model of ENzymatic Traits in Python; GitHub Repository:  
118        <https://github.com/bioatmosphere/DEMENTPy>) is a spatially and mechanistically explicit trait-  
119        and individual-based microbial systems modelling framework built upon its predecessor  
120        DEMENT (**Allison 2012; Allison 2014; Allison and Goulden 2017; Wang and Allison 2019**).  
121        This model randomly initializes a microbial community on a spatial grid based on physiological  
122        traits and simulates its dynamics by modelling explicitly demographic processes of each  
123        population including cell metabolism and growth, mortality, and reproduction at a daily time step.  
124        Driven by temperature and moisture, the community secretes different exoenzymes decomposing  
125        different organic compounds. Starting from continuous physiological traits, DEMENTpy bridges  
126        across scales from individual through community to systems in soil microbiome (see **Supporting**  
127        **Fig. 1** for model structure). Below only community initialization and intra-cellular metabolic  
128        allocation are highlighted. More details with respect to structure, processes, formula, and  
129        parameters are referred to the **Supporting Information**.

130        With a trait-based approach, DEMENTpy creates a microbial community composed of a  
131        large number of hypothetical taxa by randomly drawing values from uniform distributions of  
132        microbial traits and assigning them to different taxa (see a list of traits in **Supporting Fig. 1B** and  
133        more details in **Supporting Text**). The traits include rates of enzyme production (constitutive and  
134        inducible) and rates of osmolyte production (constitutive and inducible). Drought tolerance of each  
135        taxon is determined by normalizing the inducible osmolyte rate of production to a value from 0 to  
136        1. This formulation establishes a mechanistic connection between osmolyte production and  
137        drought tolerance (**Schimel 2007**) in contrast to the previous model version which instead directly

138 introduced a drought tolerance parameter and imposed a penalty on carbon use efficiency  
139 accordingly (**Allison and Goulden 2017**).

140 DEMENTpy explicitly treats intra-cellular metabolism of ingested monomer carbon  
141 derived from explicit exoenzymatic degradation of substrates (see the **Supporting Text** for  
142 substrate degradation and other demographic processes). The metabolic processing of assimilated  
143 carbon after growth respiration is directed to produce enzyme (and respiration) and osmolyte (and  
144 respiration; **Csonka 1989; Witteveen and Visser 1995**), which are treated as simultaneous  
145 processes without prescribing an order (**Supporting Fig. 1C**). The carbon left after these processes  
146 accumulates toward biomass. We assume the constitutive osmolyte production rate varies across  
147 taxa without depending on water potential, accounting for bacterial/fungal cell's allocation of  
148 biomass to keep a water potential balance across cell wall (**Csonka 1989**). By contrast, inducible  
149 production of osmolytes is subject to constraints from water potential only below a certain  
150 threshold. Arising from metabolic production of enzyme and osmolyte, mortality of microbial cells  
151 is simulated both deterministically by accounting for mass balance and stochastically based on  
152 death probability constrained by drought tolerance and water potential.

## 153 **2.2 Modelling experiments**

154 We applied DEMENTpy to the grassland system at Loma Ridge, Southern California  
155 (**Allison et al. 2013**) and parameterized the model with 100 different hypothetical bacterial taxa  
156 on a 100 by 100 spatial grid decomposing grass litter containing ten different substrates (see  
157 parameter values in **Supporting Table 1** and substrates in **Supporting Table 2**). DEMENTpy was  
158 benchmarked with the daily weather data of year 2011, which is treated as the ambient scenario  
159 (**Supporting Fig. 2A**).

160 On top of this ambient scenario we conducted simulations with manipulated drought to  
161 examine drought legacies (**Supporting Fig. 2**). Two drought scenarios, moderate and severe, were  
162 created by reducing the water potential across only the dry season by a factor of four and ten,  
163 respectively. After the drought period, the ambient scenario was re-imposed to examine changes  
164 in microbial communities degrading substrates. One set of such simulations without dispersal is  
165 referred to as default mode. Another set in dispersal mode is set to further examine how dispersal  
166 affects drought legacy

167 **2.3 Simulation protocol and data analysis**

168 With the model setup as above, we conducted simulations following the protocol as follows  
169 (**Supporting Fig. 2**): each simulation was run for 10 years at a daily time step after establishing  
170 an initial microbial community on the spatial grid with homogeneously distributed substrates, and  
171 in each new year substrates, monomers, and enzymes were reinitialized uniformly to have the same  
172 configurations as the very first year except for the microbial community. For the default mode,  
173 microbial community on the spatial grid in each new year was randomly reinitialized based on  
174 frequency of each taxon on the grid in the last day of the previous year (**Supporting Fig. 2C**). In  
175 contrast, in the dispersal mode the frequency was based on cumulative biomass of each taxon  
176 across the previous whole year (**Supporting Fig. 2D**). These simulations were repeated for each  
177 scenario under the two modes (default and dispersal mode) for 40 times with 40 different seeds.  
178 This sample size was determined by a convergence analysis of DEMENTpy's stochastic nature  
179 (**Supporting Fig. 3**).

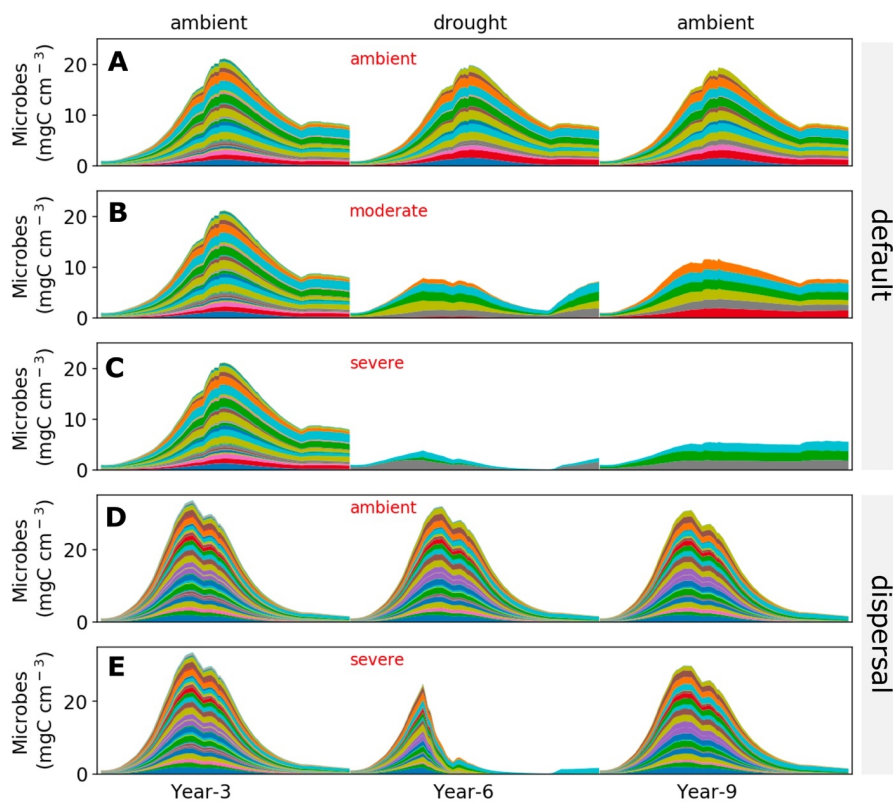
180 All results presented in this work, unless notified otherwise, were analyses of such an  
181 ensemble of 40 runs for each of the five scenarios (5×40 = 200 runs in total). A dataset was  
182 established from these simulations encompassing taxon traits (enzyme investment and drought

**Commented [SDA3]:** Why are there not 6 scenarios: ambient, moderate, and severe with default and limited dispersal?

**Commented [BW4R3]:** The reason I did not do moderate scenario for the dispersal mode is that during my earlier explorations low-intensity drought cannot have any legacy effects. so, I just did the severe scenario, arguing that since a severe scenario does not show any effects, it should be enough to support our idea.

183 tolerance), time-series of taxon-specific biomass, and time-series of community-level carbon  
184 allocation (enzymes, osmolytes, and yield), as well as time-series of compound-specific and total  
185 substrates. With taxon traits and biomass biomass-weighted community-level traits, enzyme  
186 investment and drought tolerance, were calculated (see the **Supporting Text** for calculation  
187 method). In addition, 95% confidence intervals were presented in most of the cases except for  
188 microbial community composition and community carbon allocation, for which results of only one  
189 out of the 40 simulations were shown.

190



191

192 **Fig.1. Microbial community dynamics disturbed by drought of differing severities with and**  
193 **without dispersal.** (A-C) Dynamics without dispersal under ambient, moderate, and severe  
194 scenario, respectively. (D, E) Dynamics with dispersal under ambient and severe scenario,  
195 respectively. Colored bands represent different hypothetical taxa in terms of biomass ( $\text{mg C cm}^{-3}$ )  
196 averaged over the  $100 \times 100$  spatial grid. Data shown are only for years 3, 6 (the 3<sup>rd</sup> year under  
197 drought), and 9 (the 3<sup>rd</sup> year after drought). See **Supporting Fig. 2** for the full 10-year dynamics  
198 under the ambient scenario of both default and dispersal mode.

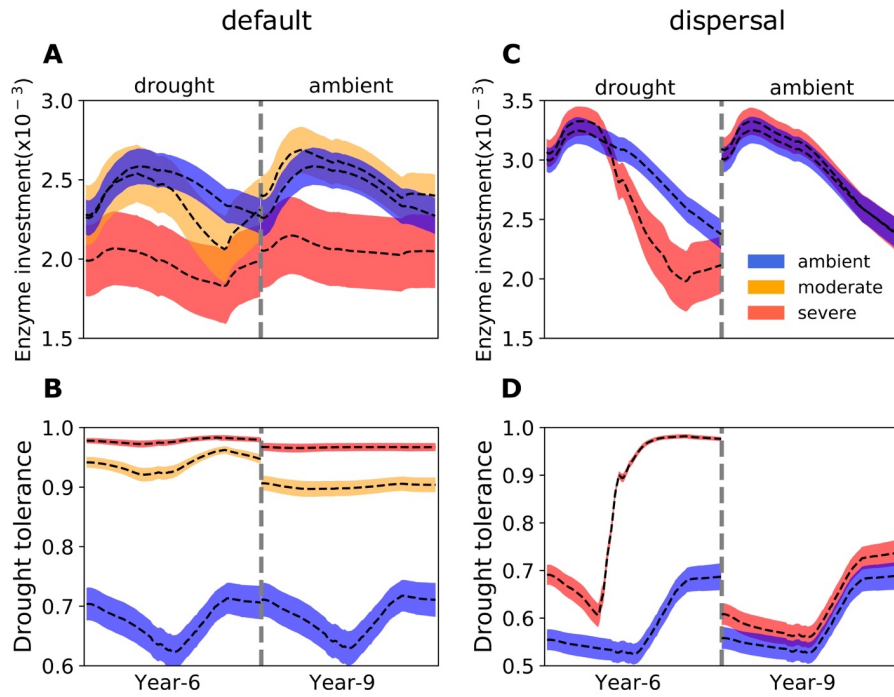
199

### 200 **3 Results**

#### 201 **3.1 Microbial community dynamics under the ambient drought scenario**

202 The system became relatively stable after 2 years, with seasonal dynamics in the microbial  
203 community repeating across years (**Supporting Fig. 2**). Seasonal dynamics with respect to  
204 community composition and biomass reflected a joint control by environment and substrates.  
205 Starting from the wet season that was replete with substrates, a microbial community consisting  
206 of different taxa established and grew in biomass. As substrates were degraded and depleted,  
207 microbial cells began to starve and die. Increasing drought while entering the dry season induced  
208 more death. These two processes in combination resulted in the decline of microbial biomass after  
209 a biomass peak around  $20 \text{ mg C cm}^{-3}$  (**Fig. 1A**) and drove the composition toward taxa with higher  
210 drought tolerance and lower enzyme investment (**Supporting Fig. 4A**) and hence community level  
211 enzyme investment decrease (**Fig. 2A**) and drought tolerance increase across the dry season **Fig.**  
212 **2B**). Similar seasonal and inter-annual dynamics were observed for the community with dispersal  
213 but with much higher biomass (peaked around  $30 \text{ mg C cm}^{-3}$ ) and taxonomic diversity (**Fig. 1D**;  
214 **Supporting Fig. 4B; Fig. 2C, D**).

215



216

217 **Fig.2 Seasonal dynamics of community-level enzyme investment and drought tolerance of**  
 218 **microbial communities under different drought scenarios. (A, B)** Enzyme investment and  
 219 drought tolerance during year 6 (3<sup>rd</sup> year under drought) and year 9 (3<sup>rd</sup> year after drought) under  
 220 three scenarios (ambient, moderate, and severe) without dispersal, respectively. **(C, D)** The same  
 221 for communities with dispersal under two scenarios (ambient and severe). Dashed lines and color  
 222 bands are means and confidence intervals (95%) based on 40 runs of each of the 5 scenarios.

223

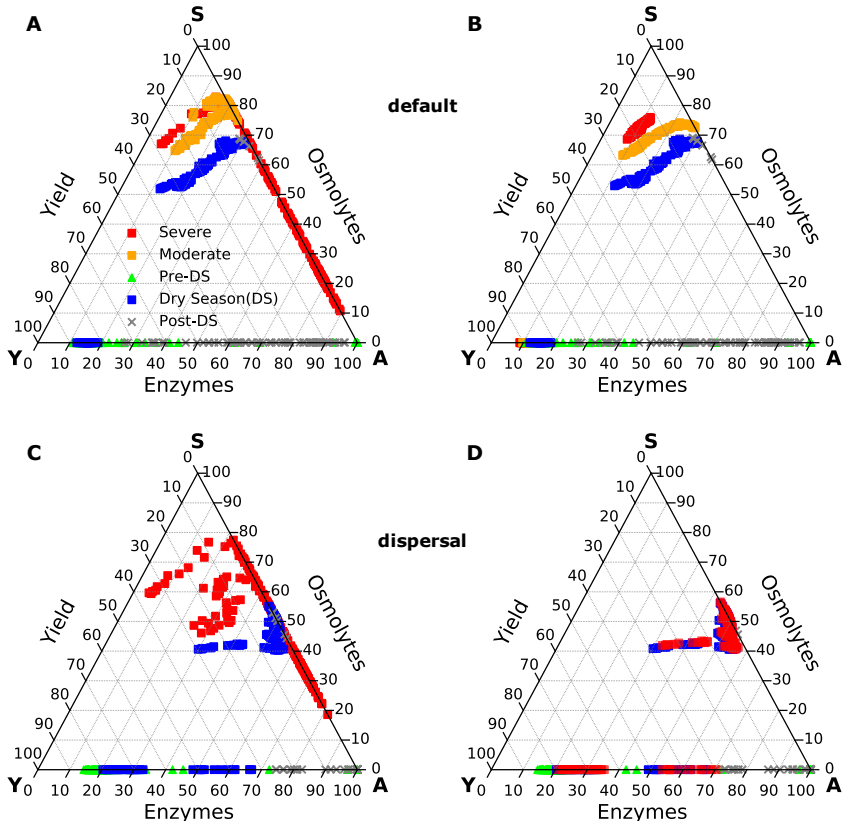
224

225

226 **3.2 Responses to and recoveries from drought disturbance of varying severity**

227 Variation in drought severity altered the microbial community to varying extents (**Fig. 1B,**  
228 **C**). Total biomass declined significantly, with the severe scenario declining the most by about 50%  
229 to a peak less than 10 mg C cm<sup>-3</sup>. Composition of the communities changed dramatically in terms  
230 of taxonomic richness and abundance, forming new alternative stable communities after 2 years  
231 of drought perturbation with differing levels of drought tolerance and enzyme investment.  
232 Compared to the ambient scenario, drought tolerance increased significantly across the whole  
233 season from as low as only 0.62 to 0.92 of the moderate scenario and to 0.97 of the severe (**Fig.**  
234 **2A,B**). However, the community enzyme investment only declined significantly in the severe  
235 scenario across the dry season and did not change much in the moderate scenario on average  
236 besides the later stage in dry season (**Fig. 2A,B**). These trait changes dictated differences in  
237 community-level carbon allocation between enzymes and osmolytes and thus yield (**Fig. 3A**).  
238 Under the moderate scenario, the percentage of assimilated carbon allocated to osmolytes ranged  
239 between 65–85%, compared to the ambient range of 50–70%, whereas enzyme allocation was  
240 consistently lower (10% on average) than the ambient (20% on average). However, the resulting  
241 yield was basically similar, ranging between 0 - 30%, though a few points in the ambient were  
242 higher (reaching at most 40%) early in the drought season. Under the severe scenario, the  
243 percentage of osmolytes became even higher and enzymes even lower, and the community yield  
244 approached zero more often. Eventually, these differences in community resource allocation  
245 between osmolytes and enzymes were manifested in the dampened degradation of substrates over  
246 the grid, with the two drought scenarios resulting in different levels of decomposition declines  
247 (average of 57.39 and 85.65%, respectively; **Fig. 4A, B**).

248



249

250 **Fig. 3** Ternary plots of community-level allocation of assimilated carbon among enzymes,  
 251 osmolytes, and yield over time under different drought scenarios. (A, B) Enzyme-Osmolyte-  
 252 Yield tradeoff of communities during year 6 (3<sup>rd</sup> year under drought) and year 9 (3<sup>rd</sup> year after  
 253 drought), respectively, of the default mode (without dispersal). (C, D) The same for the dispersal  
 254 mode. The Y, A, and S (based on the Y-A-S framework) labeled at corners correspond to yield,  
 255 enzymes, and osmolytes, respectively. Besides the ambient cases in default and dispersal mode

**Commented [BW5]:** I later found it hard to color-code the points by water potential values, as the three scenarios can overlap which make it hard to tell their differences.

Instead, I changed the color for the ambient of pre-dry season. Since the focus is on dry season, for which the current visualization should be able to tell the general pattern among them.

But I am open to further explore more options.

256 illustrating the whole season, moderate and severe scenarios were only shown during the dry  
257 season. See **Supporting Fig. 2C** for calculations of enzymes, osmolytes, and yield.

258

259 Once the ambient conditions were re-imposed, after 2 years (year 9) new stable microbial  
260 communities formed (**Fig. 1B, C** and **Supporting Fig. 2C**). Compared to the ambient scenario,  
261 these newly-formed communities had different drought tolerance and enzyme investment (**Fig. 2A,**  
262 **B**). Drought tolerance was significantly higher under both the moderate (0.90) and severe scenario  
263 (0.96) than under the ambient, though both became a little lower than the communities realized  
264 under drought disturbance. In contrast, enzyme investment under the moderate scenario became  
265 similar to the ambient community, with only the severe scenario community remaining  
266 significantly different. Only the severe community showed a clearly lower allocation to enzymes  
267 than the ambient community across the dry season (**Fig. 3B**). This loss of differences in enzyme  
268 investment in the moderate community eventually resulted in only the severe scenario displaying  
269 significantly reduced degradation compared to the ambient scenario (by 47.72% on average; **Fig.**  
270 **4B**), although the magnitude of decline was dampened compared to the antecedent drought period  
271 because of the relief of drought pressure (**Fig. 4A**). It is noteworthy that prior to year 9, the  
272 degradation changes resulting from the transient communities (year 7) were significant for both  
273 drought scenarios (an average decline by 18.00 and 55.52%, respectively).

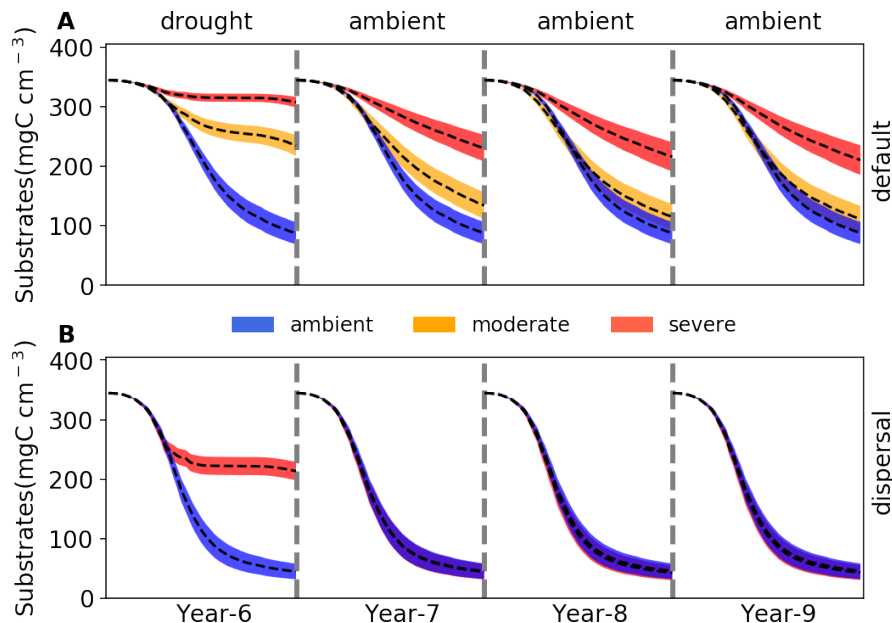
274

275

**Commented [SDA6]:** I hesitate to call them alternative stable states here because we do not present data after year 9 to demonstrate stability.

**Commented [BW7R6]:** i actually did 10-yr simulations, and starting from year 3, the system all basically stabilized. I did not present those considering the supporting fig. 2 sort of justifies this.

I temporarily still use the persistent term throughout the ms. one option could be to add a few lines explaining this issue, e.g., in the methods section?



276

277 **Fig. 4 Changes in substrates driven by drought.** (A) Total substrates on the spatial grid over  
278 year 6-9 under three different scenarios (ambient, moderate, and severe) without dispersal. (B) The  
279 same for simulations with dispersal under ambient and severe scenarios. Dashed lines and colored  
280 bands are means and confidence intervals (95%), respectively, based on 40 runs for each of the  
281 five scenarios. See **Supporting Fig. 5** for an example illustration of the underlying substrate-  
282 specific changes.

283

284 **3.3 Responses to and recoveries from the severe drought disturbance with dispersal**

285 With dispersal the microbial community realized under the severe scenario saw both lower  
286 total biomass and lower taxonomic abundance, particularly significant during the dry season (**Fig.**  
287 **1E**). This stable community realized under severe drought had significantly different community

288 enzyme investment and drought tolerance from the ambient. Enzyme investment declined from  
289 0.0033 to 0.0020 and drought tolerance increased sharply from 0.60 to 0.97 across the dry season,  
290 increasing their differences from ambient over time (**Fig. 2C,D**). These changes resulted in the  
291 community allocating more assimilated carbon to produce osmolytes and less to enzymes, which  
292 resulted in zero yield when drought was most severe during the dry season (**Fig. 3C**). All these  
293 changes pointed to significant declines in decomposition of substrates (an average decline of  
294 56.29%; **Fig. 4C**)

295 However, when ambient conditions were re-imposed, recovery from drought was rapid.  
296 After 2 years, the community became similar to the ambient (**Fig. 1E**). This compositional  
297 similarity coincided with similar community enzyme investment (**Fig. 2C**) and drought tolerance  
298 (**Fig. 2D**), which resulted in the same community-level allocation of assimilated carbon among  
299 enzymes (30 - 60%), osmolytes (40 - 60%), and thus yield (0 – 30%; **Fig. 3D**). These similarities  
300 eventually had the almost completely same substrates' decomposition (**Fig. 4D**). In fact, in contrast  
301 to the default mode, the transient community did not show significant effects in the very 1<sup>st</sup> year  
302 after drought (year 7; **Fig. 4D**). This was attributed to the fact that the community became same  
303 immediately after the drought.

304

#### 305 **4 Discussion**

306 With trait-based modelling in a mechanistically explicit fashion, this study examined the  
307 relationships between drought legacy and drought severity and dispersal in simulated litter  
308 microbiomes. Manifestation of drought legacy at the system level in terms of litter decomposition  
309 was contingent on drought severity and microbial dispersal, forming an array from persistent  
310 through transient to no legacy at all (**Fig. 4**). Such a wide set of legacy scenarios with respect to

311 property, magnitude, and duration point to a more overarching, fundamental mechanistic basis  
312 underpinning drought legacy in soil microbiome—physiological tradeoff between enzyme and  
313 drought tolerance.

314 Clearly, the severity of drought disturbance matters in the magnitude and duration of legacy  
315 formed via determining the extent to which a microbial community can adapt. By increasing the  
316 drought intensity we revealed legacies from transient to persistent (**Fig. 4A**). It is easy to expect  
317 no legacy at all if with an even weaker disturbance, which we did not cover in the current study.  
318 All these simulations were based on an assumption of a realization of stable state under drought  
319 disturbances. We argue this assumption is a reasonably good starting point, which in reality is not  
320 always the case for sure considering huge variation in frequency, intensity, and/or duration of  
321 drought.

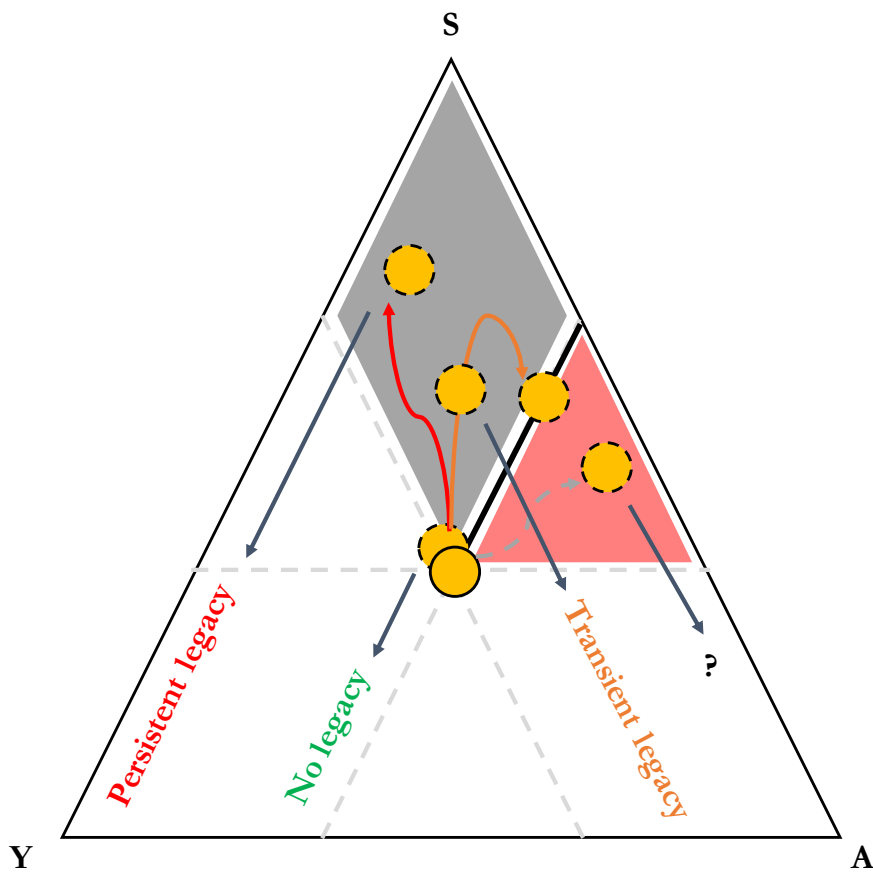
322 Drought disturbance of a relatively low severity, though being able to result in a declined  
323 decomposition after disturbance conferred by the transient community, eventually saw a  
324 disappearance of the legacy effect (**Fig. 4A**), which we dub transient legacy. This transient legacy  
325 matches the field rainfall manipulative experiment with a reciprocal design at the same site very  
326 well, which observed mitigated drought legacy in terms of litter decomposition within three years  
327 (**Martiny et al. 2017**). It is noteworthy that this transient legacy arose from an eventual community  
328 with the same functioning but different composition and biomass. However, a role of biomass  
329 difference can be excluded for leading to this decomposition indifference, as indicated by the peak  
330 biomass decline by as high as 50% under the moderate scenario (**Fig. 1B**). This exclusion of  
331 biomass change in contributing to legacy formation is consistent with findings from both a field  
332 manipulative experiment at Loma Ridge, Southern California (**Martiny et al. 2017**) and a  
333 reciprocal transplant study across a climate gradient in Southern California (**Glassman et al. 2019**).

334 Therefore, the loss of legacy fundamentally resulted from the remaining same community enzyme  
335 investment (accompanied by a realization of higher community drought tolerance) after a  
336 relatively less intense drought disturbance (**Fig. 2A,B**). Such a compositional but not functional  
337 change in the new stable alternative system reflects a broad notion of functional similarity in the  
338 soil microbiome (**Allison and Martiny 2008**), which has been widely observed across natural  
339 systems (e.g., **Ives & Carpenter 2007; Fukami 2015**).

340 In contrast, persistent drought legacy (**Fig. 4B**) can be shaped by a stronger drought  
341 disturbance that can push the community to reach an even higher drought tolerance by sacrificing  
342 more of capability in enzyme investment, thereby forming a community not only compositionally  
343 but also functionally different (**Fig. 2A,B**). A similar long-term legacy but expressed in soil  
344 heterotrophic respiration was also observed by microcosm and field transplant experiments by  
345 **Hawkes et al. (2017)**. More generally, historical contingency of alternative stable system with a  
346 functional difference has been widely reported across different systems with disturbances beyond  
347 drought, e.g., in gut microbiota experiencing transient osmotic perturbation (**Tropini et al. 2018**)  
348 and in forest biome across tropical (**Hirota et al. 2011; Staver et al. 2011**) and boreal forest  
349 (**Herzschuh 2019**), as well as in small pond systems (**Chase 2003**).

350 However, microbial communities shaped by legacy of varying drought disturbance,  
351 though being able to last and carry the legacy effects into the future, are faced with other  
352 disturbances and thereby should be subject to changes. Our simulations demonstrated that dispersal  
353 is one such process that can negate formation of even transient legacy in organic matter  
354 decomposition. By constantly introducing taxa from the same microbial pool, we found that  
355 dispersal under even the severe drought scenario can completely mitigate the physiological  
356 tradeoff-mediated drought selection on a microbial community (**Fig. 1E**). As a result of community

357 similarities in drought tolerance and enzyme investment (**Fig. 2C,D; Fig. 3D**), dispersal can  
358 overwhelm the drought legacy in organic matter decomposition (**Fig. 4B**). We must acknowledge  
359 that factors in dispersal influencing resident community are manifold (**Vila et al. 2019**); for  
360 instance, timing (i.e., priority effects; **Fukami 2015**) and velocity (**Evans et al. 2019**) both have  
361 been suggested to be important. Moreover, even an unsuccessful dispersal with only transient  
362 interactions can induce an alternative stable state functioning differently (**Amor et al. 2020**).  
363 Therefore, the scenario examined in this study (with a purpose of revealing underlying  
364 mechanisms) by no means is exclusive; for example, with passive dispersal in a field transplant  
365 experiment **Hawkes et al. (2017)** did not find any apparent mitigation of historical rainfall legacy  
366 in soil respiration. Therefore, responding to the huge variation in the dispersal process, a microbial  
367 community could instead present compositional and functional changes to varying extents (e.g.,  
368 **Fukami 2015**) and hence varying magnitudes of legacy in decomposition, which warrant more  
369 explorations.



370

371 **Fig. 5 Drought legacy contingent on the trajectory of a microbial community on the Y-A-S**  
 372 **space.** There will be no legacy if a community does not move at all or move along the thick black  
 373 line. Instead, if the community moves into and stays in the grey region, persistent legacy will occur.  
 374 However, if the community eventually leaves the grey region and settles on the thick black line,  
 375 only transient legacy can occur. However, it is speculated to have another trajectory of a

376 community moving into the red region with both increased drought tolerance and enzyme  
377 investment.

378

379 From the contrasts of cases of low vs. high drought severity (transient vs. persistent legacy)  
380 and of cases with vs. without dispersal (no legacy vs. persistent legacy), we can arguably deduce  
381 that drought legacy in microbiome functioning originates from physiological tradeoff between  
382 enzyme and osmolyte production and is eventually determined by the position that a community  
383 can reach on its potential space constrained by enzyme investment, drought tolerance, and yield  
384 (**Fig. 5**). For instance, when drought forces the community to move to a position of higher drought  
385 tolerance but eventually similar enzyme investment (e.g., low level drought as shown in the  
386 moderate scenario; **Fig. 4A**), only transient legacy occurs. When the community does not move at  
387 all on the space (e.g., with dispersal present under even a relatively severe drought; **Fig. 4B**), even  
388 transient legacy may not be able to appear. In contrast, when a community shift towards an  
389 increasing abundance of drought-tolerant taxa by sacrificing capacity of enzyme production  
390 enables its move to a position of higher drought tolerance and lower enzyme investment (e.g.,  
391 under an intense drought as shown in the severe scenario; **Fig. 4A**), persistent legacy in impaired  
392 capability in degrading substrates can occur.

393 With this reasoning, any agent that is capable of shaping the trajectory of a community on  
394 the Y-A-S constrained space may influence the property, magnitude, and/or duration of drought  
395 legacy. In fact, mechanisms and factors influencing strength of the tradeoff between enzyme and  
396 osmolyte can be complex and manifold. Tradeoffs in microbiome and beyond are complex in  
397 general (e.g., **Berezovsky & Shakhnovich, 2005; Ferenci 2016**); notably, tradeoffs are not  
398 necessarily rigid, which may even be the opposite of a tradeoff (e.g., **Tikhonov et al. 2020**). Such

399 complexities can be induced by factors including, among others, drought intensity, dispersal, and  
400 potentially many others and processes including, e.g., metabolic plasticity and evolution. For  
401 instance, we speculate a fourth scenario of both increased drought tolerance and enzyme  
402 investment that emerges from a loss of enzyme-osmolyte tradeoff under certain conditions, which  
403 in theory is possible as long as without breaking the constraint of tradeoff with yield (**Fig. 5**).  
404 Therefore, broadening the scope of scenarios examined in this study (as discussed earlier) and/or  
405 relaxing assumptions in DEMENTpy offers natural directions in which our study can be extended  
406 for enriching the tradeoff-mediated mechanisms underpinning drought legacy. This tradeoff notion  
407 raises a broad question of how to pinpoint soil microbiomes in spaces constrained by traits' space.  
408 Extending this tradeoff-mediated drought legacy mechanism to larger spatial scales across  
409 different systems would be a path to address this question, which is expected to be a fruitful  
410 research avenue. It is highly expected that insights gained from these tradeoff strength-oriented  
411 inquiries not only can reconcile the huge discrepancies across studies in different systems with  
412 respect to property, magnitude, and duration but also would uncover tempo-spatial patterns in the  
413 long run.

414 In summary, tradeoff-mediated drought legacies emerging from trait-based microbial  
415 community shifts bear immediate implications for understanding soil microbiome and broad  
416 consequences for quantifying ecosystems' responses and feedbacks to increasing frequency and  
417 severity of drought and other environmental changes. Through cell metabolic plasticity in terms  
418 of resource allocation between enzyme and osmolyte microbial communities achieve self-  
419 organization after drought disturbances to reach different states. This notion can be totally  
420 extended to any other disturbances that soil microbiome faces. Thereby, this insight arguably  
421 points to next step efforts of leveraging rich -omics information to better inform such plasticity

422 expressed in physiological traits at single cell level (e.g., **Hatzenpichler et al. 2020**). Moreover, a  
423 more accurate quantification of drought legacy with this tradeoff-based mechanism enables a  
424 better evaluation of their interactions with vegetation for addressing ecosystem dynamics and  
425 functioning. For instance, even a transient legacy of impaired decomposition may enhance carbon  
426 sequestration in soil systems at certain temporal scales, but may also allow fuels to accumulate for  
427 the next fire season, thereby increasing fire risk (e.g., **Pellegrini et al. 2017**). Additionally,  
428 impaired decomposition can inhibit release of nutrients from detritus and thus their return to plants,  
429 influencing plant-microbe interactions (e.g., **Legay et al. 2018**). All these and potentially many  
430 other cascading changes arising from microbiome legacy would engender more complex  
431 feedbacks in ecosystems. Evaluating their implications entails an integrative, holistic view of  
432 components in systems across ecosystem and the Earth System scales. To proceed, this study  
433 clearly indicates that to really establish a predictive science of ecosystems in the context of  
434 projected global climate change, considering history as an essential component means that  
435 dimensions and spaces of essential tradeoffs distilled from tremendous taxonomic diversity should  
436 be incorporated. This trait-based modelling of soil microbiome, together with progress in trait-  
437 based insights into vegetation, offer an inspirational starting point for moving forward in this  
438 direction.

439

#### 440 **References**

- 441 Allison, S. D. (2012). A trait-based approach for modelling microbial litter decomposition.  
442 Ecology letters, 15, 1058-1070.

443

- 444 Allison, S. D., Lu, Y., Weihe, C., Goulden, M. L., Martiny, A. C., Treseder, K. K., & Martiny, J.  
445 B. (2013). Microbial abundance and composition influence litter decomposition response to  
446 environmental change. *Ecology*, 94, 714-725.
- 447
- 448 Berezovsky, I. N., & Shakhnovich, E. I. (2005). Physics and evolution of thermophilic adaptation.  
449 *Proceedings of the National Academy of Sciences*, 102, 12742-12747.
- 450
- 451 Birch, H. F. 1958. The effect of soil drying on humus decomposition and nitrogen availability.  
452 *Plant and Soil*, 10, 9–31.
- 453
- 454 Borsa, A. A., Agnew, D. C., & Cayan, D. R. (2014). Ongoing drought-induced uplift in the western  
455 United States. *Science*, 345, 1587-1590.
- 456
- 457 Conradi, T., Van Meerbeek, K., Ordonez, A., & Svenning, J. C. (2020). Biogeographic historical  
458 legacies in the net primary productivity of Northern Hemisphere forests. *Ecology Letters*.  
459 <https://doi.org/10.1111/ele.13481>
- 460
- 461 Csonka, L. N. (1989). Physiological and genetic responses of bacteria to osmotic stress.  
462 *Microbiological Reviews*, 53, 121-147.
- 463
- 464 Cuddington, K. (2011). Legacy Effects: The Persistent Impact of Ecological Interactions.  
465 *Biological Theory*, 6, 203–210.
- 466

- 467 Evans, S.E., Wallenstein, M.D. (2012) Soil microbial community response to drying and rewetting  
468 stress: does historical precipitation regime matter? *Biogeochemistry*, 109, 101–116.
- 469
- 470 Falkowski, P. G., Fenchel, T., & Delong, E. F. (2008). The microbial engines that drive Earth's  
471 biogeochemical cycles. *Science*, 320, 1034-1039.
- 472
- 473 Ferenci, T. (2016). Trade-off mechanisms shaping the diversity of bacteria. *Trends in  
474 Microbiology*, 24, 209-223.
- 475
- 476 Gommers, P. J. F., Van Schie, B. J., Van Dijken, J. P., & Kuenen, J. G. (1988). Biochemical limits  
477 to microbial growth yields: an analysis of mixed substrate utilization. *Biotechnology and  
478 Bioengineering*, 32, 86-94.
- 479
- 480 Green, J.K., Seneviratne, S.I., Berg, A.M. *et al.* (2019). Large influence of soil moisture on long-  
481 term terrestrial carbon uptake. *Nature*, 565, 476–479.
- 482
- 483 Herzschuh, U. (2020). Legacy of the Last Glacial on the present-day distribution of deciduous  
484 versus evergreen boreal forests. *Global Ecology and Biogeography*, 29, 198-206
- 485
- 486 Hinojosa, M. B., Laudicina, V. A., Parra, A., Albert-Belda, E., & Moreno, J. M. (2019). Drought  
487 and its legacy modulate the post-fire recovery of soil functionality and microbial community  
488 structure in a Mediterranean shrubland. *Global Change Biology*, 25, 1409-1427.
- 489

- 490 Hobbie, J. E., & Hobbie, E. A. (2013). Microbes in nature are limited by carbon and energy: the  
491 starving-survival lifestyle in soil and consequences for estimating microbial rates. *Frontiers in*  
492 *Microbiology*, 4, 324.
- 493
- 494 Johnstone, J. F., Allen, C. D., Franklin, J. F., Frelich, L. E., Harvey, B. J., Higuera, P. E., ... &  
495 Schoennagel, T. (2016). Changing disturbance regimes, ecological memory, and forest resilience.  
496 *Frontiers in Ecology and the Environment*, 14, 369-378.
- 497
- 498 Karhu, K., Auffret, M., Dungait, J. *et al.* (2014) Temperature sensitivity of soil respiration rates  
499 enhanced by microbial community response. *Nature*, 513, 81–84
- 500
- 501 López-Urrutia, Á., & Morán, X. A. G. (2007). Resource limitation of bacterial production distorts  
502 the temperature dependence of oceanic carbon cycling. *Ecology*, 88, 817-822.
- 503
- 504 Manzoni, S., Schimel, J. P., & Porporato, A. (2012). Responses of soil microbial communities to  
505 water stress: results from a meta-analysis. *Ecology*, 93, 930-938.
- 506
- 507 Meisner, A., Rousk, J., & Bååth, E. (2015). Prolonged drought changes the bacterial growth  
508 response to rewetting. *Soil Biology and Biochemistry*, 88, 314-322.
- 509
- 510 Sardans, J., & Peñuelas, J. (2010). Soil enzyme activity in a Mediterranean forest after six years  
511 of drought. *Soil Science Society of America Journal*, 74, 838-851.
- 512

513 Schimel, J., Balser, T. C., & Wallenstein, M. (2007). Microbial stress-response physiology and its  
514 implications for ecosystem function. *Ecology*, 88, 1386-1394.

515

516 Schimel, J. P., & Weintraub, M. N. (2003). The implications of exoenzyme activity on microbial  
517 carbon and nitrogen limitation in soil: a theoretical model. *Soil Biology and Biochemistry*, 35,  
518 549-563.

519

520 Sinsabaugh, R. L., Manzoni, S., Moorhead, D. L., & Richter, A. (2013). Carbon use efficiency of  
521 microbial communities: stoichiometry, methodology and modelling. *Ecology Letters*, 16, 930-939.

522

523 Tiemann, L. K., & Billings, S. A. (2011). Changes in variability of soil moisture alter microbial  
524 community C and N resource use. *Soil Biology and Biochemistry*, 43, 1837-1847.

525

526 Wang, B., & Allison, S. D. (2019). Emergent properties of organic matter decomposition by soil  
527 enzymes. *Soil Biology and Biochemistry*, 136, 107522.

528

529 **Acknowledgements**

530 All data and code underlying the analyses and illustrations in this manuscript are archived

531 at: <https://github.com/bioatmosphere/microbiome-drought-legacy>. DEMENTPy code is available

532 at <https://github.com/bioatmosphere/DEMENTPy>.

1 Supporting Information

2 **Tradeoff-mediated Drought Legacy in Soil Microbiome**

3 Bin Wang, Steven D. Allison

4

5 **1 DEMENTpy**

6 DEMENTpy, a trait-based explicit microbial systems modelling framework both  
7 mechanistically and spatially, is an effort of mechanistically updating (see **Supporting Fig. 1** for  
8 conceptual structure) and programmatically restructuring (see **Supporting Fig. 6** for programming  
9 structure) DEMENT that was initially developed in 2012 (**Allison 2012**). The source code in  
10 Python is archived at <https://github.com/bioatmosphere/DEMENTPy>. Processes simulated in  
11 DEMENTpy are described below.

12 **1.1 Microbial community initialization**

13 With a trait-based approach, a microbial pool comprises a large number of hypothetical  
14 taxa in DEMENTpy is created by randomly drawing values from distributions of various microbial  
15 and enzymatic traits (**Supporting Table 1**) and assigning them to different taxa. These  
16 hypothetical taxa in the microbial pool with differing combinations of trait values are randomly  
17 placed on the spatial grid to form a spatially-explicit microbial community. See animations at  
18 <https://bioatmosphere.github.io/DEMENTPy/> to get an intuitive notion of this spatial feature, and  
19 an application of this feature to addressing enzymatic heterogeneity scaling in **Wang and Allison**  
20 (**2019**). Trait distributions are all assumed to follow uniform distributions, except that for  
21 simplicity, some traits are assumed to be constants, and values of some traits are derived from  
22 established correlations with other traits. These distributions and assumptions are largely informed  
23 by field- and lab-based experimental works (**Allison 2012; Allison and Goulden 2017**).

24       Four of the major traits determining intra-cellular metabolism of enzyme and osmolyte and  
25      thus mass balance are rates of enzyme production (constitutive and inducible) and rates of  
26      osmolyte production (constitutive and inducible). On top of these rates, taxon-specific number of  
27      genes encoding different enzymes and osmolytes are determined randomly under the constraint of  
28      systems setup. Therefore, rate and number together determine amounts of enzyme and osmolyte a  
29      cell can produce. The rate of production of inducible osmolyte is then normalized to a value from  
30      0 to 1, which is regarded as drought tolerance. Such a treatment of drought tolerance is an update  
31      to the previous version which instead directly introduced a drought tolerance parameter and  
32      imposed a penalty on carbon use efficiency accordingly (**Allison and Goulden 2017**). Starting  
33      from osmolyte production to determine drought tolerance is supposed to be more biologically  
34      realistic (**Schimel 2007**). Additionally, a whole set of enzymatic traits including Vmax and Km  
35      of both enzyme and transporter is employed to explicitly parameterize a certain number of different  
36      enzymes and transporters allowed in a system.

37 **1.2 Metabolic production of enzyme and osmolyte**

38       Different individuals (hypothetical taxa) comprising the microbial community complete  
39      their demographic processes of growth, mortality, and reproduction while degrading substrates  
40      and ingesting monomers under the influence of temperature and water potential. From these  
41      underlying processes emerges dynamics and functioning at both the microbial cell level and the  
42      whole system level.

43       Degradation of substrates are calculated explicitly by using different enzymes with  
44      different kinetic properties. One principle during the simulation is that every substrate at least has  
45      one enzyme to degrade and vice versa. Different monomers are calculated explicitly by having  
46      differing transporters to target them. Transporters of different types and amounts are taxon-specific,

47 which is described immediately below. The governing equation of both substrates' degradation  
48 and monomers' uptake follows the Michaelis-Menten equation, which is further constrained by  
49 temperature (accounting for temperature impacts on enzymatic kinetics) and water potential  
50 (accounting for enzymatic kinetics and diffusion declines arising from drought; **Allison and**  
51 **Goulden 2017**):

52

53

54

55

56 where  $E$  and  $S$  represent enzyme and substrate concentration, respectively,  $V_{max}$  represents the  
57 enzyme catalytic constant,  $K_m$  denotes the concentration of  $S$  at which  $V$  is one half  $V_{max}$ ,  $\varepsilon$  is  
58 enzymatic activation energy,  $R$  is universal gas constant, and  $k$  is a coefficient controlling water  
59 potential sensitivity that distinguishes between degradation and uptake.

60 Intra-cellular production of enzymes and osmolytes are described below in detail with  
61 respect to simulation methods and their underlying rationales. Cellular metabolism explicitly deals  
62 with both the carbon upon uptake from degraded substrates and the carbon in biomass of microbial  
63 cells inducibly and constitutively (**Supporting Fig. 3**). The metabolic processing of assimilated  
64 carbon after growth respiration (constrained by a constant) is directed to enzyme (and respiration)  
65 and osmolyte production (and respiration; **Csonka 1989; Witteveen and Visser 1995**), which are  
66 treated horizontally in the model without prescribing an order. The carbon left after these processes  
67 accumulates toward biomass. We assume the constitutive osmolyte production rate ( $Osmo\_Con$ )  
68 varies across taxa without depending on water potential, accounting for bacterial/fungal cell's  
69 allocation of biomass to keep a water potential balance across cell wall (**Csonka 1989**). In contrast,

70 taxon-specific inducible production of osmolytes ( $O_{ind}$ ) is subject to constraints from water  
71 potential and is calculated following:

72

73  $\alpha$

74

75 where  $O_{ind}$ , indexed by taxon i, is the  $i^{th}$  taxon's inducible osmolyte production rate,  $\psi$  is the daily  
76 water potential,  $\alpha$  is a water potential coefficient, and  $\theta$  is a system water potential constant, below  
77 which inducible osmolyte production is activated. Though with a differing production rate across  
78 taxa, osmolyte in the current version without differentiating among different compounds is  
79 assumed to hold a constant stoichiometry of C/N = 3, which governs consumption of N in  
80 intracellular metabolism. This ratio is based on an average of the three most common osmotic  
81 compounds in bacteria (Csonka 1989): proline (C5H9NO2), glycine betaine (C5H11NO2), and  
82 glutamine (C5H10N2O3).

83 Arising from metabolic production of enzyme and osmolyte, mortality of microbial cells  
84 is simulated both deterministically by accounting for mass balance relative to a threshold and  
85 stochastically based on death probability constrained by drought tolerance and water potential.  
86 Here the taxon-specific mortality probability ( $Mort$ ) is calculated following:

87

88

89

90 where  $\beta$  is  $i^{th}$  taxon's basal mortality probability,  $\gamma$  is a water potential coefficient,  $\delta$  is  $i^{th}$  taxon's  
91 drought tolerance, and  $\theta$  is a system water potential constant. Microbial cells that are either out of  
92 mass balance or randomly killed are designated as dead ones, removed from the microbial

93 community, and added into the substrates pools as dead microbes. Microbial reproduction is  
94 simply calculated by splitting microbes into two halves, which disperse to surrounding grid boxes  
95 on the spatial grid.

96

97 **2. Community-level traits**

98 Community-level enzyme investment ( $E_{com}$ ) and drought tolerance ( $D_{com}$ ) weighted by  
99 biomass are calculated as:

100

101

102 respectively, where  $E_i$  and  $D_i$  refer to the  $i^{th}$  taxon's enzyme production rate and drought tolerance,  
103 respectively, and  $M_i$  is the relative biomass of the  $i^{th}$  taxon in the community.

104

105 **References**

106 Allison, S. D. (2012). A trait-based approach for modelling microbial litter decomposition.  
107 Ecology letters, 15, 1058-1070.

108

109 Allison, S. D., & Goulden, M. L. (2017). Consequences of drought tolerance traits for microbial  
110 decomposition in the DEMENT model. Soil Biology and Biochemistry, 107, 104-113.

111

112 Bugmann, H., Fischlin, A., & Kienast, F. (1996). Model convergence and state variable update in  
113 forest gap models. Ecological Modelling, 89, 197-208.

114

115 Wang, B., & Allison, S. D. (2019). Emergent properties of organic matter decomposition by soil  
116 enzymes. Soil Biology and Biochemistry, 136, 107522.

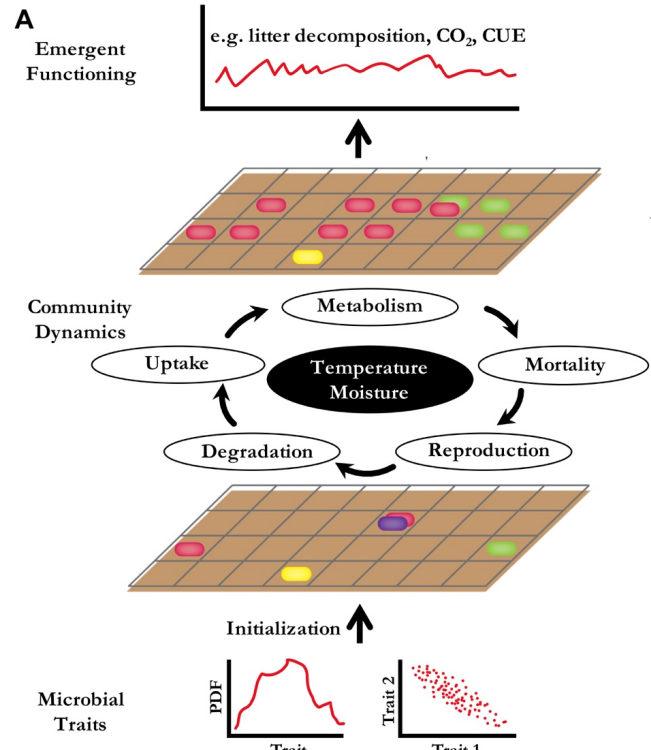
**Supporting Table 1** Major microbial and enzyme parameters and their values

Parameter	Value	Unit	Note
max_size_b	2	mg cm <sup>-3</sup>	C quota threshold for bacterial cell division
Cfrac_b	0.825	mg mg <sup>-1</sup>	Bacterial C fraction
Nfrac_b	0.16	mg mg <sup>-1</sup>	Bacterial N fraction
Pfrac_b	0.015	mg mg <sup>-1</sup>	Bacterial P fraction
Crangle	0.09	mg mg <sup>-1</sup>	Tolerance on C fraction
Nrange	0.04	mg mg <sup>-1</sup>	Tolerance on N fraction
Prange	0.005	mg mg <sup>-1</sup>	Tolerance on P fraction
C_min	0.086	mg cm <sup>-3</sup>	threshold C concentration for cell death
N_min	0.012	mg cm <sup>-3</sup>	threshold P concentration for cell death
P_min	0.002	mg cm <sup>-3</sup>	threshold C concentration for cell death
Uptake_C_cost_min	0.01	transporter mg <sup>-1</sup> biomass C	Minimum per enzyme C cost as a fraction of uptake
Uptake_C_cost_max	0.1	transporter mg <sup>-1</sup> biomass C	Maximum per enzyme C cost as a fraction of uptake
Uptake_Maint_cost	0.01	mg C transporter <sup>-1</sup> day <sup>-1</sup>	Respiration cost of uptake transporters
Enz_per_taxon_min	0		Minimum number of enzymes a taxon can produce
Enz_per_taxon_max	40		Maximum number of enzymes a taxon can produce
Enz_Prod_min	0.00001	mg C mg <sup>-1</sup> day <sup>-1</sup>	Minimum per enzyme production cost as a fraction of C uptake rate
Enz_Prod_max	0.0001	mg C mg <sup>-1</sup> day <sup>-1</sup>	Maximum per enzyme producton cost as a fraction of C uptakte rate
Constit_Prod_min	0.00001	mg C mg <sup>-1</sup> day <sup>-1</sup>	Minimum per enzyme production cost as a fraction of biomass C
Constit_Prod_max	0.0001	mg C mg <sup>-1</sup> day <sup>-1</sup>	Maximum per enzyme production cost as a fraction of biomass C
Osmo_per_taxon_min	1		Minimum number of osmolyte a taxon can produce
Osmo_per_taxon_max	1		Maximum number of osmolyte a taxon can produce
Osmo_Consti_Prod_min	0.0000001	mg C mg <sup>-1</sup> day <sup>-1</sup>	Minimum per osmolyte production cost as a fraction of biomass C
Osmo_Consti_Prod_max	0.000001	mg C mg <sup>-1</sup> day <sup>-1</sup>	Maximum per osmolyte production cost as a fraction of biomass C
Osmo_Induci_Prod_min	0.01	mg C mg <sup>-1</sup> day <sup>-1</sup>	Minimum per osmolyte production cost as a fraction of C uptake rate
Osmo_Induci_Prod_max	0.1	mg C mg <sup>-1</sup> day <sup>-1</sup>	Maximum per osmolyte production cost as a fraction of C uptake rate
CUE_ref	0.5	mg mg <sup>-1</sup>	Growth efficiency at the reference temperature
CUE_temp	-0.005	mg mg <sup>-1</sup>	Growth efficiency change with enzyme investment
death_rate_bac	0.001		Bacterial death rate
basal_bac	10		Bacterial basal death probability
wp_th	-2		water potential threshold at which osmolyte is induced
alpha	0.01		Osmolyte production change with water potential
Vmax0_min	5	mg substrate mg <sup>-1</sup> enzyme day <sup>-1</sup>	Minimum Vmax for enzyme
Vmax0_max	50	mg substrate mg <sup>-1</sup> enzyme day <sup>-1</sup>	Maximum Vmax for enzyme

Uptake_Vmax0_min	1	mg substrate mg-1 substrate day-1	Minimum uptake Vmax
Uptake_Vmax0_max	10	mg substrate mg-1 substrate day-1	Maximum uptake Vmax
Uptake_Ea_min	35	kJ mol-1	Minimum activation energy for uptake
Uptake_Ea_max	35	kJ mol-1	Maximum activation energy for uptake
Km_min	0.01	mg cm-3	Minimum Km
Uptake_Km_min	0.001	mg cm-3	Minimum uptake Km
Vmax_Km	1	mg enzyme day cm-3	Slope for Km-Vmax relationship
Vmax_Km_int	0	mg cm-3	Intercept for Km-Vmax relationship
Uptake_Vmax_Km	0.2	mg biomass day cm-3	Slope for uptake Km-Vmax relationship
Uptake_Vmax_Km_int	0	mg cm-3	Intercept for uptake Km-Vmax relationship
Specif_factor	1		Efficiency-specificity

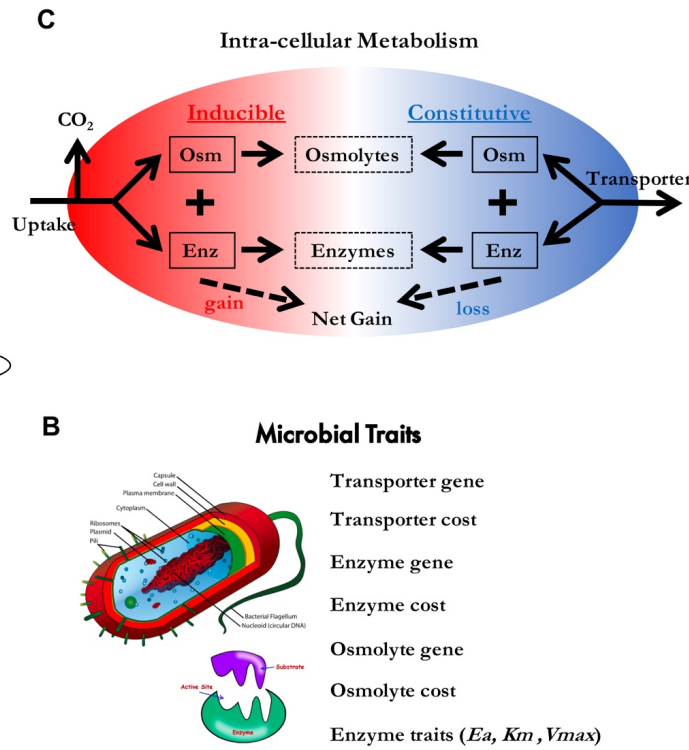
**Supporting Table 2** Substrate concentrations initialized in DEMENT simulations (mg cm<sup>-3</sup>).

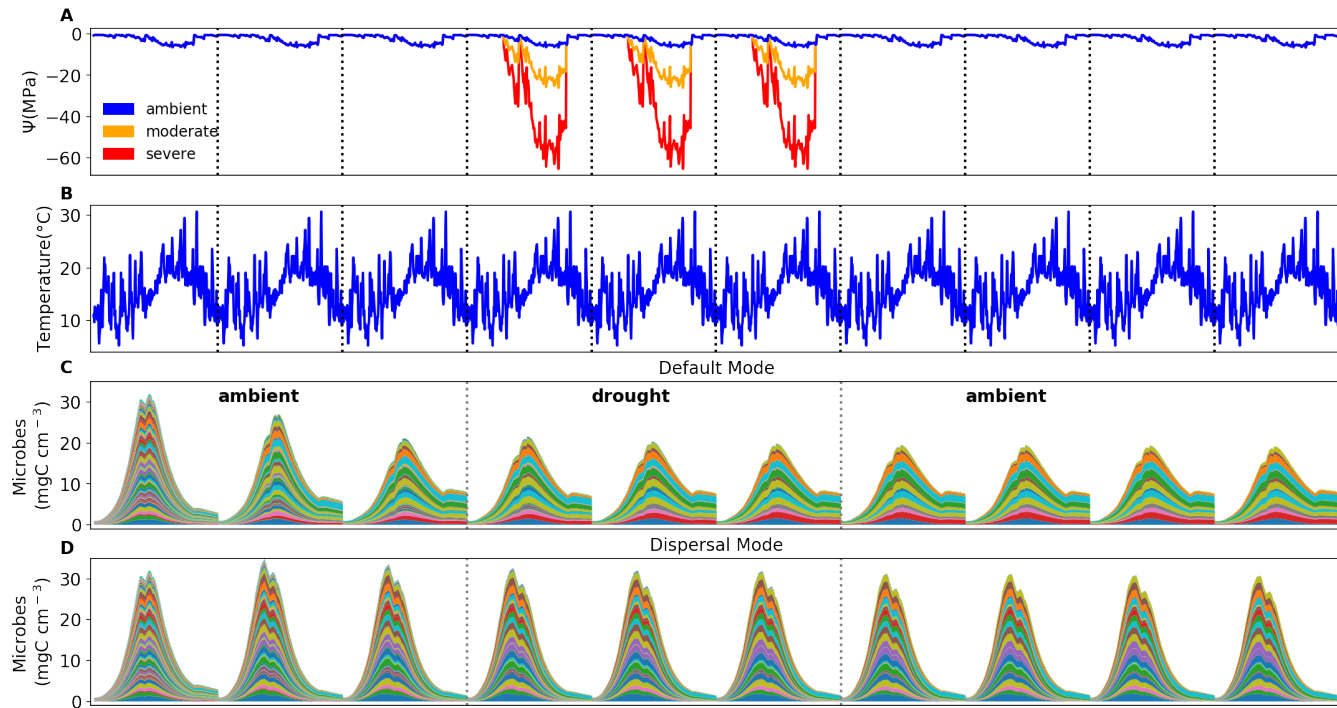
Substrate	C	N	P
DeadMic	0	0	0
DeadEnz	0	0	0
Cellulose	146.89	0	0
Hemicellulose	85.855	0	0
Starch	12.21	0	0
Chitin	4.9952	0.83254	0
Lignin	48.51	0.40425	0
Protein1	10.6	2.09704	0
Protein2	10.6	2.09704	0
Protein3	10.6	2.09704	0
OrgP1	12.48	0	0.478469
OrgP2	1.8182	0.79745	0.478469



119

120 Supporting Fig. 1 DEMENTpy conceptual structure and underpinning traits and intra-cellular metabolism.

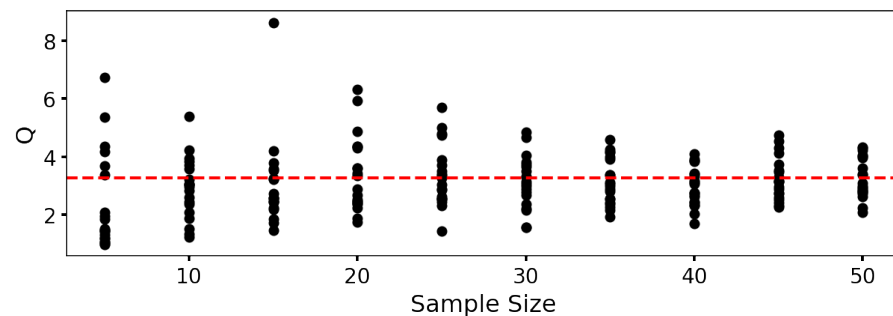




121

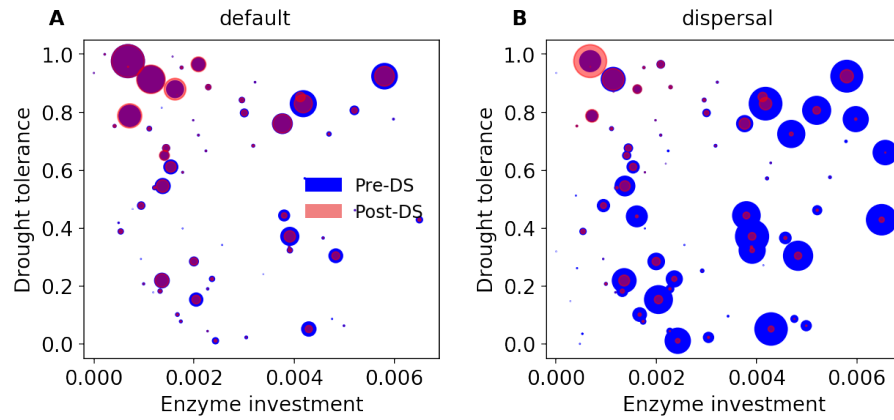
122 **Supporting Fig. 2 Environmental forcing and microbial community dynamics.** (A) Ambient daily water potential of 2011, with the  
 123 orange and red line denoting the moderate and severe drought scenario, respectively, which are manipulated values simply by  
 124 multiplying the water potential across the dry season (from April through September) by 4 and 10, respectively. (B) The corresponding  
 125 daily temperature. (C, D) Microbial community dynamics of the default vs. dispersal mode over 10 years under the ambient drought

126 scenario. The simulation experiences three phases as separated by the dashed grey lines: a spin-up phase of three years to realize a  
127 relatively stable community; a disturbance phase of imposing different drought scenarios for three years; and a final recovery phase  
128 after drought disturbance. Colored bands represent different hypothetical taxa.



129

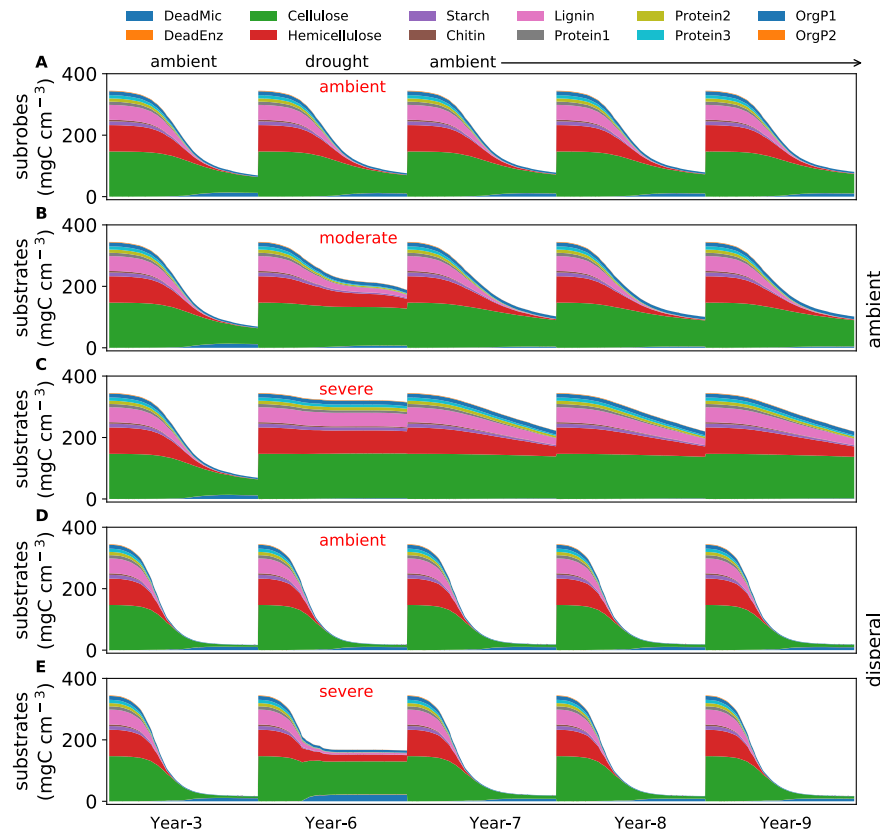
130 **Supporting Fig. 3 DEMENTpy (v1.0) stochasticity convergence analysis.** Q (quotient) is  
 131 calculated as (90% percentile - 10% percentile)/median with the data of degradation of substrates  
 132 following Bugmann et al. (1996). Each sample size has 20 replicates that were randomly drawn  
 133 from a sample pool of 112 runs. This analysis illustrates that a sample size of 40, which starts  
 134 displaying relatively stabilized and converged variation, may be an appropriate choice considering  
 135 a tradeoff of reliability vs. consumption of computing resource.



136

137 **Supporting Fig. 4 Taxonomic changes in traits across dry season.** (A) Taxon-specific traits of  
 138 drought tolerance and enzyme investment of a microbial community without dispersal before (blue)  
 139 and after the dry season (red) under the ambient scenario. (B) The same for a microbial community  
 140 with dispersal. Each point corresponds to a different taxon, and the size is proportional to its  
 141 biomass.

142



143

144 **Supporting Fig. 5 Substrate-specific dynamics under differing drought scenarios. (A, B, C)**

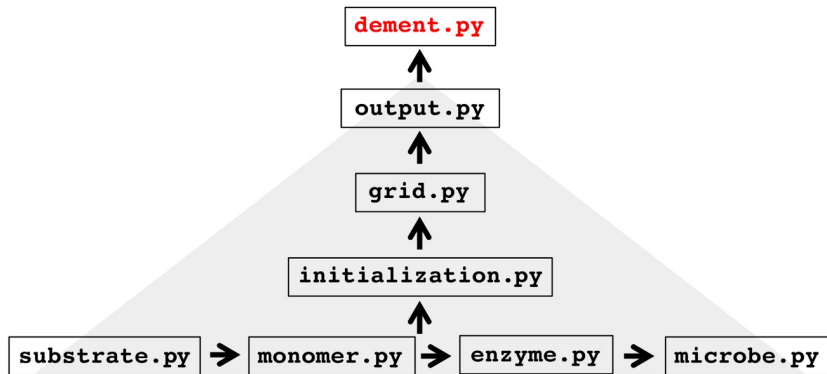
145 the dynamics under ambient, moderate, and severe scenarios in default mode for year 3 and year

146 6 (the 3<sup>rd</sup> year under drought disturbance) through year 9. (D, E) the same for the dispersal mode

147 but with only ambient and severe scenarios. Each color band represents one type of 12 different

148 substrates.

## DEMENTpy Programming Structure



Hierarchically designed w/ 8 modules  
Spatially- & metabolism-explicit



149

150 Supporting Fig. 6. DEMENTpy programming structure. DEMENTpy emerges from  
151 hierarchically restructuring and mechanistically updating DEMENT programmed in R.